NRC Research Press

ARTICLE

Soil compressibility in transient unsaturated seepage analyses

Timothy D. Stark, Navid H. Jafari, Aaron L. Leopold, and Thomas L. Brandon

Abstract: Most levee underseepage and uplift analyses are based on steady-state seepage and can yield conservative results. Although computations are simpler and steady-state seepage parameters are easier to determine and readily available, transient unsaturated seepage analyses are more representative of levee seepage conditions because boundary conditions acting on the levee or floodwall and saturation change with time, which induce pore-water pressure and seepage changes with time in the embankment and foundation strata. In addition, these boundary conditions, e.g., flood surge or storm event, are rapid such that steady-state conditions may not have time to develop in the embankment and some foundation materials. Transient seepage analyses using a floodwall case study indicate that as soil compressibility of the underseepage layer decreases, rapid landside pore-water pressures increase and can approach steady-state values. The transient results also indicate that uplift factors of safety during the flood event are about 22% higher than those at steady state. The effect of soil compressibility can delay or accelerate the onset of uplift water pressure increase from the initial steady-state conditions.

Key words: transient seepage analysis, hydraulic conductivity, coefficient of volume compressibility, compressibility, levee, hydraulic gradient, uplift, coefficient of consolidation, slope stability.

Résumé : La plupart des analyses de l'écoulement et du soulèvement des digues sont basées sur l'écoulement en régime permanent et peuvent donc donner des résultats conservateurs. Malgré que les calculs soient plus simples et que les paramètres en régime permanent soient plus faciles à déterminer et disponibles, les analyses d'écoulement en régime transitoire sont plus représentatives des conditions d'écoulement des digues puisque les conditions frontières qui agissent sur la digue ou sur le mur d'endiguement de même que la saturation varient avec le temps, ce qui entraîne des variations temporelles des pressions interstitielles et de l'écoulement dans le remblai et dans les couches de fondation. De plus, ces conditions frontières, par exemple une inondation ou une tempête, sont rapides, donc les conditions du régime permanent peuvent ne pas avoir le temps de se développer dans le remblai et dans certains matériaux de fondation. Des analyses d'écoulement transitoire faites sur le cas d'un mur d'endiguement indiquent que lorsque la compressibilité du sol de la couche sous l'écoulement diminue, les pressions interstitielles associées à un glissement de terrain rapide augmentent et peuvent approcher les valeurs en régime permanent. Les résultats transitoires indiquent aussi que les facteurs de sécurité du soulèvement durant l'inondation sont environ 22 % plus élevés qu'en régime permanent. L'effet de la compressibilité du sol peut retarder ou accélérer le déclenchement de l'augmentation de la pression d'eau de soulèvement à partir des conditions initiales en régime permanent. [Traduit par la Rédaction]

Mots-clés : analyse d'écoulement transitoire, conductivité hydraulique, coefficient de compressibilité volumique, compressibilité, digue, gradient hydraulique, soulèvement, coefficient de consolidation, stabilité de pente.

Introduction

Over 100 000 miles of flood protection infrastructure are currently operating in the United States, e.g., along the Mississippi, Sacramento, Trinity, Missouri, and American rivers. The increase in development behind levees and floodwalls poses increased risk to public health and safety. The societal, economic, and environmental risks will consequently play a greater role in assessing the required performance of flood protection. Current performance of urban levees and floodwalls to hurricane and flood events are primarily based on steady-state seepage analyses. By assuming steady-state seepage, Bennett (1946) was able to develop closed-form solutions to evaluate the quantity of landside underseepage, uplift pressures, and hydraulic gradients. The U.S. Army Corps of Engineers (USACE) design manuals EM 1110-2-1901 and EM 1110-2-1913 (USACE 1993, 2000) adopted the Bennett (1946) approach. This method and the manuals represent the state of practice for evaluating landside hydraulic gradients and uplift pressures from levee underseepage.

Hurricane and flood conditions typically only act for a period of hours to weeks, which may not allow sufficient time to develop steady-state conditions (Peter 1982). As a result, a transient seepage analysis, e.g., wetting front or other movement of water in unsaturated soil, provides a more realistic approach to evaluating levee seepage and slope stability, especially in failure causation analyses (Li and Desai 1983; Lam et al. 1987; Lane and Griffiths 2000).

Lambe and Whitman (1969) define transient flow as the condition during water flow where pore-water pressure, and thus total head, changes with time. During transient conditions, changes in hydraulic boundary conditions and boundary total stresses cause (*i*) saturated seepage through relatively pervious foundation strata (Casagrande 1937, 1961; Mansur et al. 1956, 2000; Turnbull and Mansur 1961; Wolff 1974, 1989; Daniel 1985; Chapuis and Aubertin 2001), (*ii*) unsaturated seepage through earth embankments (Cooley 1983; Lam and Fredlund 1984; Zaradny 1993; Chen and Zhang 2006; Le et al. 2012), and (*iii*) shear-induced pore-water pressures

Received 16 July 2013. Accepted 13 January 2014.

T.D. Stark, N.H. Jafari, and A.L. Leopold. Department of Civil and Environmental Engineering, University of Illinois at Urbana-Champaign, 205 N. Mathews Ave., Urbana, IL 61801-2352, USA.
T.L. Brandon. Department of Civil and Environmental Engineering, Virginia Tech, 22 Patton Hall, Blacksburg, VA 24061, USA.
Corresponding author: Navid Jafari (e-mail: njafari2@illinois.edu).

resulting from changes in boundary total stresses, e.g., flood water or storm surge (Paton and Semple 1961; Kulhawy et al. 1969; Desai 1972; Nobari and Duncan 1972; Duncan et al. 1990; Berilgen 2007; Pinyol et al. 2008; Alonso and Pinyol 2011).

The first change (saturated seepage) depends on the saturated horizontal hydraulic conductivity (k_h), hydraulic conductivity anisotropy (ratio of vertical k to horizontal k or k_v/k_h), and coefficient of volume compressibility (m_v; hereafter referred to as soil compressibility) of embankment and foundation strata through which underseepage will occur. The second mechanism (unsaturated seepage) relies on unsaturated hydraulic conductivity function and soil-water characteristic curves (Fredlund and Rahardjo 1993) and causes delays in seepage and propagation of pore-water pressures. This effect is less influential for the floodwall case study presented herein because seepage occurs in the initially saturated foundation strata and hence is not discussed further. In the third mechanism (total stresses), positive pore-water pressures resulting from changes in shear and normal stresses are not calculated in a transient analysis. For example, shear-induced pore-water pressures from sudden drawdown after a prolonged flood stage can result in the upstream slope becoming unstable. This problem requires a coupled analysis of flow and stress deformation analysis using a constitutive soil model. The transient seepage analyses performed using commercial finite element analysis (FEA) programs are uncoupled from changes in total stress. Therefore, shear and normal stress induced pore-water pressures are not considered in this paper.

The impact of steady-state conditions and foundation underseepage on earth structures is well documented (e.g., Mansur and Kaufman 1957; Turnbull and Mansur 1961; Wolff 1974, 1989, 2002; Cunny 1980; Daniel 1985; Cedergren 1989; Gabr et al. 1996;). However, the influence of soil compressibility on underseepage and uplift pressures is less understood by geotechnical engineers. Browzin (1961), Brahma and Harr (1962), Newlin and Rossier (1967), Desai and Sherman (1971), and Desai (1972, 1977) present transient seepage analyses, but the models do not consider m_v and assume only saturated flow. Borja and Kishnani (1992) consider slow drawdown but assume steady-state pore-water pressure conditions at different reservoir levels.

This paper demonstrates the importance of soil compressibility in transient seepage analyses, presents methods for evaluating and selecting compatible values of m_v, and provides recommendations for performing transient and unsaturated seepage analyses for levees and floodwalls. This paper uses a calibrated floodwall case study to show the influence of m_v on landside uplift pressures during flood and hurricane events.

Seepage theory

This section briefly summarizes transient seepage theory, the importance of m_v, and provides methods for determining m_v. Freeze and Cherry (1979) present detailed derivations of m_v and transient seepage equations, which are summarized in the following text. The equation for three-dimensional transient flow through a saturated anisotropic porous medium is

$$(1) \qquad \frac{\partial}{\partial x}\left(k_x\frac{\partial h_t}{\partial x}\right) + \frac{\partial}{\partial y}\left(k_y\frac{\partial h_t}{\partial y}\right) + \frac{\partial}{\partial z}\left(k_z\frac{\partial h_t}{\partial z}\right) = S_s\frac{\partial h_t}{\partial t}$$

where k is the hydraulic conductivity in the x, y, and z directions, h_t is the total hydraulic head, t is time, and S_s is the specific storage. Specific storage is expressed as $S_s = \gamma_w(m_v + n\beta)$, where γ_w is the unit weight of water, n is porosity, and β is compressibility of water. Because water is incompressible (4.7×10^{-7} kPa^{-1}) for seepage purposes, specific storage reduces to $S_s = \gamma_w m_v$.

Time is introduced in the seepage analysis via the right-hand side (RHS) of eq. (1). For a unit decline in total hydraulic head, the RHS is directly related to the magnitude of m_v. If an incompressible value of m_v of 1×10^{-7} kPa^{-1} is assumed, the RHS approaches zero, which corresponds to a steady-state seepage condition shown in eq. (2). Consequently, the steady-state seepage analysis becomes independent of time and generates landside pore-water pressures and gradients significantly higher, e.g., equivalent to a steady-state analysis, by only decreasing the parameter m_v.

$$(2) \qquad \frac{\partial}{\partial x}\left(k_x\frac{\partial h_t}{\partial x}\right) + \frac{\partial}{\partial y}\left(k_y\frac{\partial h_t}{\partial y}\right) + \frac{\partial}{\partial z}\left(k_z\frac{\partial h_t}{\partial z}\right) = 0$$

Water flow occurs due to changes in total head, phreatic surface, and compression of the saturated seepage layer, i.e., specific storage (Rushton and Redshaw 1979; Holtz and Kovacs 1981). Of the three mechanisms, only changes in total head and specific storage are included in eq. (1). Phreatic surface is a function of unsaturated soil properties and hydraulic boundary condition, e.g., flood hydrograph. Because the time-variant nature of seepage problems is generally due to movement of the phreatic surface, the compression of the saturated seepage layer can be neglected, i.e., specific storage is negligible (Rushton and Redshaw 1979). However, m_v in eq. (1) influences transient flow by controlling the rate of pore-water pressure response in saturated layers. Therefore, applying reasonable values of m_v for the saturated seepage layer is important and determines if pore-water pressures, and thus gradients, can be rapidly transmitted to the landside.

Table 1 summarizes m_v values for soils and rocks, which generally range from 1×10^{-3} to 1×10^{-8} kPa^{-1}, respectively. The compressibility of sound rock as well as sandy gravel is similar to water and thus assumed to be incompressible. Representative m_v values for fine-grained soils, e.g., soft organic clays and peats to stiffer overconsolidated clays and tills, are also provided in Table 1. The compressibility of soils found near floodplains, i.e., normally consolidated alluvial clays given in Table 1, fall within a range of 3×10^{-4} to 1.5×10^{-3} kPa^{-1}. This narrow range of m_v influences pore-water pressure transmission through saturated foundation strata and is investigated herein using a floodwall case study.

Estimating soil compressibility

Soil compressibility describes the strain induced under an applied effective vertical stress (σ'_v) and is related to the constrained modulus (D) of the soil, see eq. (3). The m_v value can be determined from constant rate of strain (ASTM (2012) standard D4186) or incremental loading (ASTM (2011*a*) standard D2435) one-dimensional (1-D) consolidation tests.

$$(3) \qquad m_v = \frac{\Delta\varepsilon_v}{\Delta\sigma'_v} = \frac{1}{D}$$

where ε_v is the vertical strain.

Soil compressibility can also be expressed in terms of σ'_v, initial void ratio (e_o), and slope of the e–logσ'_v relationship, i.e., the compression index, C_c, as shown in eq. (4). Values of C_c and e_o can be easily determined from results of 1-D consolidation tests on high-quality specimens.

$$(4) \qquad m_v = \frac{0.434C_c}{(1 + e_o)\sigma'_v}$$

Figures 1*a* and 1*b* provide m_v values for three fine-grained soils located in the Inner Harbor Navigation Canal (IHNC) along the Lower Ninth Ward in New Orleans, Louisiana. These values were computed from incremental load and constant rate of strain 1-D consolidation tests conducted on large-diameter (125 mm) fixed-piston samples. Figure 1*a* illustrates the general trend of m_v with

Table 1. Range of m_v for various materials (after Domenico and Mifflin 1965 and Bell 2000).

Material	m_v (kPa^{-1})
Organic alluvial clays and peats	≥1.5×10^{-3}
Normally consolidated alluvial clays	3×10^{-4} to 1.5×10^{-3}
Varved and laminated clays, firm to stiff clays	1×10^{-4} to 3×10^{-4}
Very stiff or hard clays, tills	5×10^{-5} to 1×10^{-4}
Heavily overconsolidated tills	≤5×10^{-5}
Loose sand	1×10^{-4} to 5.2×10^{-5}
Dense sand	2.1×10^{-5} to 1.3×10^{-5}
Dense sandy gravel	1×10^{-5} to 5.2×10^{-6}
Sound and jointed rock	≤6.9×10^{-6}
Water (β)	4.7×10^{-7}

Fig. 1. Compressibility (m_v) of clayey soils in terms of (*a*) natural water content and (*b*) effective vertical stress (σ'_{vo}) from laboratory consolidation tests (data from Fugro 2012).

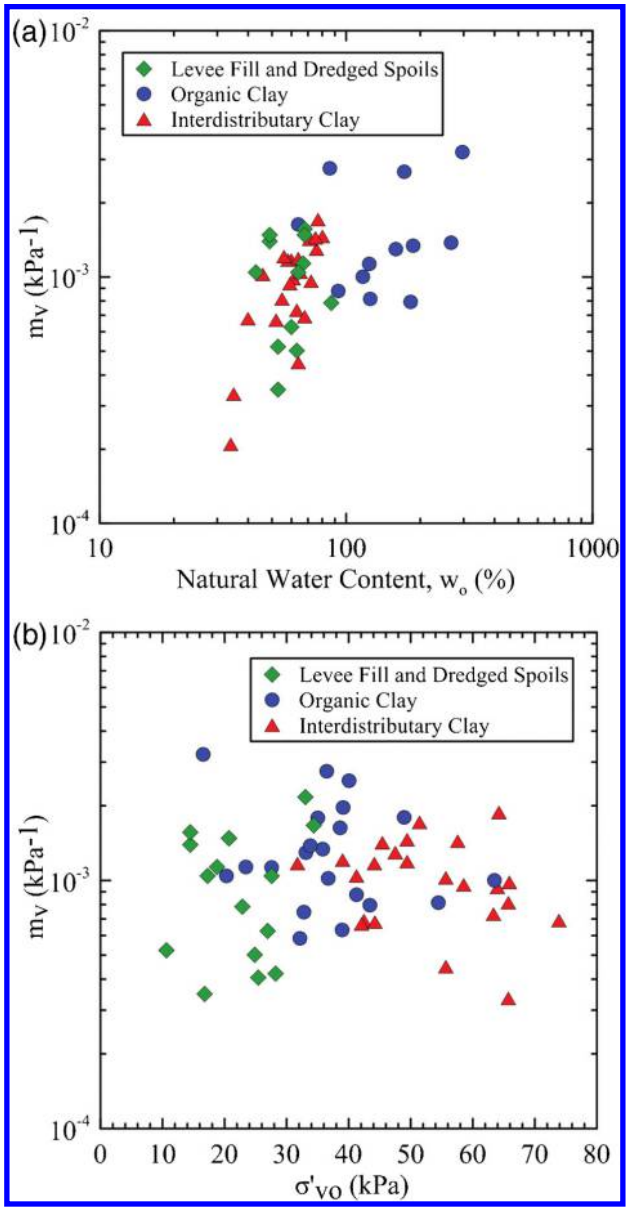

increasing natural water content (w_o), and Fig. 1*b* shows compressibility as a function of in situ σ'_{vo}. In Fig. 1*a*, the soil compressibility slightly increases as water content increases, which may be attributed to soil mineralogy changing the in situ void ratio during deposition. However, Fig. 1*b* indicates a limited correlation between m_v and σ'_{vo}. Values of m_v range from 2×10^{-4} to 2×10^{-3} kPa^{-1} for the saturated inorganic soils and from 7×10^{-4} to 3.5×10^{-3} kPa^{-1} for saturated organic clays located along the IHNC. The levee fill along the IHNC and interdistributary (ID) clay underlying the IHNC floodwall exhibit a similar range of m_v because the levee fill material was generated from dredging of the organic and ID clays to create the IHNC. The material was spread along the side of the canal to create the original levee and subsequent floodwall. The data in Fig. 1 illustrate the variability of m_v and uncertainty in selecting an appropriate value for seepage analyses. As a result, a range of m_v values should be used in transient and unsaturated seepage analyses as discussed in the following text.

If a planning level seepage analysis is desired, m_v can be estimated by obtaining an estimate of compression index (C_c) from an empirical correlation with in situ water content. For example, Fig. 2 shows compression index C_c of IHNC soils as a function of in situ water content. A direct relationship between the compression index and in situ water content exists in Fig. 2 because both are controlled by soil composition and structure (Terzaghi et al. 1996). The composition of soil, i.e., mineralogy, controls because any soil that comes to equilibrium at a high void ratio under typical overburden pressures displays high compressibility when subjected to an increase in σ'_v beyond the preconsolidation pressure, σ'_p. The IHNC organic clay deposits come to equilibrium at water contents of 100%–400% and display values of C_c typically in the range of 1–5 because a large amount of water is held within and among the organic particles (Mesri and Ajlouni 2007). The levee fill and ID clay (inorganic clays and silts) exhibit typical in situ water contents below 100% and C_c below 1. In the absence of laboratory testing on high-quality samples, Fig. 2 provides an empirical correlation between C_c and w_o for IHNC soils, i.e., $C_c = w_o/100$, that may be used to estimate m_v.

Another method to evaluate m_v is to calibrate a transient seepage model with vibrating wire (VW) piezometric data during hurricane events, storm surges, or floods. For example, the remedial work along the 17th Street Canal in New Orleans after Hurricane Katrina required installation of piezometers on both the landside and floodside of the levee. Using the recorded changes in canal level before and during Hurricane Gustav in 2010, a transient seepage analysis was developed and calibrated by modeling the piezometric response on both sides of the levee (URS 2011). Before Hurricane Gustav, the steady-state groundwater condition was matched with piezometer readings and the groundwater surface in soil borings. To replicate piezometer readings during Hurricane Gustav, both k_h and m_v were adjusted within reasonable ranges until agreement between the piezometer response and transient seepage model was achieved. As a result, the calibrated transient seepage model can be used to estimate uplift pressures during future storm surges or floods or the effectiveness of remedial measures. The estimated m_v computed for the organic clay at the 17th Street floodwall is 6.3×10^{-4} kPa^{-1}, which is in agreement with the values shown in Table 1 and Fig. 1. A similar calibration was performed for the case study using VW piezometer data during Tropical Storm Lee in 2011.

Case history and parametric analysis

Hurricane Katrina was a Category 3 hurricane when it made landfall on the Gulf Coast in 2005, with maximum sustained surface winds of 282 km/h (kph; 165 mph) (IPET 2007). The resulting tidal surge rushed from the Gulf of Mexico through the Mississippi River – Gulf Outlet (MR–GO) and the Gulf Intracoastal Waterway (GIWW) to produce a storm surge of about 4.25 m (14 ft) and wind speeds over 160 kph (100 mph) in the IHNC along the Lower Ninth Ward. This storm surge severely loaded and overtopped portions of the IHNC floodwall wall that was constructed to protect the adjacent Lower Ninth Ward. This storm surge con-

Fig. 2. Correlation between compression index and in situ water content for IHNC soils (data from Fugro 2012).

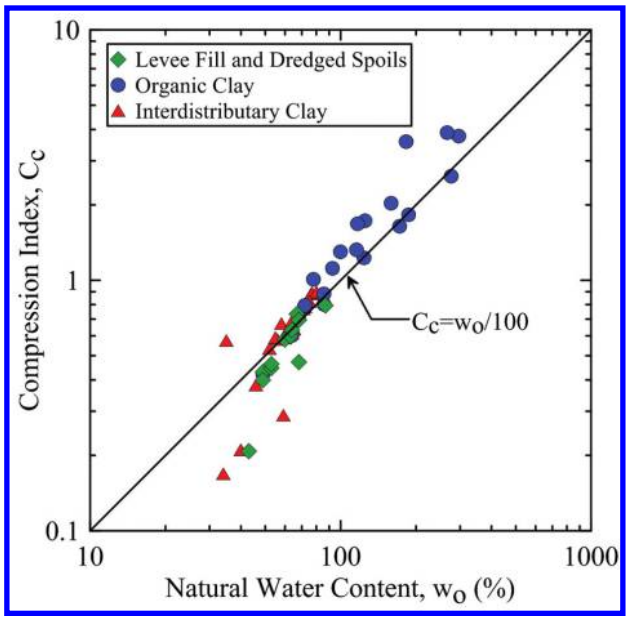

tributed to two failures of the eastern portion of the floodwall along Jourdan Avenue in the Lower Ninth Ward: (*i*) the north breach located at the north end of the Lower Ninth Ward and directly south of the Florida Avenue Bridge and (*ii*) the south breach located north of the Claiborne Avenue Bridge near the middle of the Lower Ninth Ward.

The floodwall cross section shown in Fig. 3 is located immediately south of the north breach and is denoted the "no-failure section" herein because this area of the floodwall did not fail during Hurricane Katrina. A large soil borrow pit, shown by the dashed line in Fig. 3, and filled with water prior to Hurricane Katrina, was previously excavated to acquire suitable backfill material for the various excavations created during environmental restoration of the eastern side of the IHNC (referred to as the East Bank Industrial Area (EBIA) herein). These excavations were created to remove contaminated soils, building foundations, utilities, and other infrastructure from abandoned industrial activities to allow future expansion of the IHNC. Topographic surveys (WGI 2001; Wink 2005) show the borrow pit is about 23 m (75 ft) from the floodwall and has a 3H:1V (H, horizontal; V, vertical) sideslope on the floodwall side of the excavation (see Fig. 3). The maximum depth of the borrow pit is 3.5 m, i.e., elevation –3.5 m NAVD88 (North American Vertical Datum, 1988), which is about 0.3 m (1 ft) lower than the tip of the floodwall sheet pile (elevation –3.2 m NAVD88) under the concrete portion of the floodwall. The NAVD88 corresponds to the current elevation datum in New Orleans. Figure 4 illustrates the depth of the borrow pit excavation, its close proximity to the floodwall, and the organic clay underlying the floodwall.

Cross section A–A′ in Fig. 3 shows the location of the floodwall cross section shown in Fig. 5. The cross section in Fig. 5 depicts the sheet pile-supported floodwall and three fine-grained soil layers located along the IHNC. The cross section is located in the area between the north and south floodwall breaches and through the soil borrow pit used to backfill floodside excavations created to remove contaminated soils, building foundations, utilities, and other infrastructure.

The levee fill and dredged spoils are composed of dredged organic and ID clays from creation of the IHNC that were used to construct the levee that parallels the east side of the IHNC. The fill material consists of a heterogeneous mixture of gray, soft to stiff

Fig. 3. Aerial view of large water-filled soil borrow pit excavation within 23 m of floodwall prior to Hurricane Katrina between north and south breaches (29°58′41.50″N, 90°01′14.14″W; photo courtesy of Gulf Coast Aerial Mapping, Baton Rouge, Louisiana).

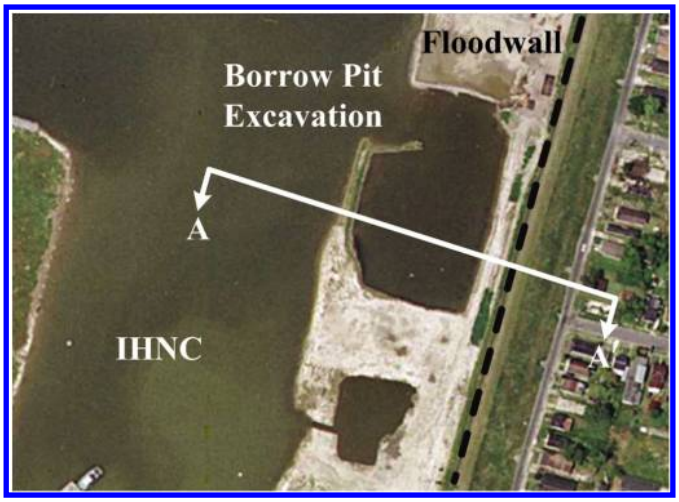

lean clay, silt, silty sand, and shell fragments. The levee fill exhibits a w_o, liquid limit (LL), and plasticity index (PI) of 43%–68%, 73%–103%, and 21%–76%, respectively, based on an extensive subsurface investigation conducted in 2011 (see Table 2). The organic clay underlying the levee fill and dredged spoils is a soft, gray to dark gray soil formed in this deltaic environment. The organic content ranges from 2% to 62%, predominantly consisting of roots and pieces of wood. The organic clay w_o, LL, and PI values range from 57% to 296%, 70% to 309%, and 46% to 196%, respectively. The ID clay consists of gray to dark gray, medium to soft clay, with lenses of silty sand and silt and medium lean clay. The ID clay w_o, LL, and PI range from 34% to 80%, 33% to 97%, and 16% to 72%, respectively. Table 2 summarizes the soil classification, saturated unit weight (γ_{sat}), w_o, LL, and PI values of these three soil layers that are used in subsequent transient seepage analyses.

The cross section through the borrow pit area in Fig. 5 is used in the following transient seepage analysis. This cross section should exhibit the shortest underseepage path and quickest storm surge response along this portion of the IHNC because the borrow pit was not backfilled prior to Hurricane Katrina. The derivation of transient seepage flow in eq. (1) indicates that m_v can influence the time required to reach increased pore-water pressures, which increases generation of seepage forces and uplift at the landside levee toe. Thus, the no-failure case study is used herein to establish the role of soil m_v on landside pore-water pressure by performing a parametric analysis using k_h, m_v, and levee geometry. The parametric analyses use uplift factor of safety (FS) — the ratio of total stress and pore-water pressure at the top of organic clay layer to evaluate floodwall performance. This site consists mainly of fine-grained soils so there is limited potential for uplift failure at the toe. However, the procedure used to calculate the uplift pressures is instructive for other sites containing fine-grained soils overlying pervious foundations.

Transient model

The two-dimensional SEEP/W finite element program (Geo-Slope International 2007) was used to model groundwater conditions and underseepage along the IHNC, including the cross section in Fig. 5. The SEEP/W program is a general seepage analysis program formulated to model saturated and unsaturated transient flow through soil and excess pore-water pressure dissipation estimated from a stress deformation analysis within porous materials. The SEEP/W program can model different hydraulic conductivities,

Fig. 4. Excavation of soil borrow pit located within 23 m of floodwall and 3.5 m deep, showing organic clay that underlies floodwall (photo from WGI 2005).

Fig. 5. Floodwall cross section through borrow pit used for parametric seepage analysis that shows sheet pile supported floodwall, initial phreatic surface, and landside backfilled excavation.

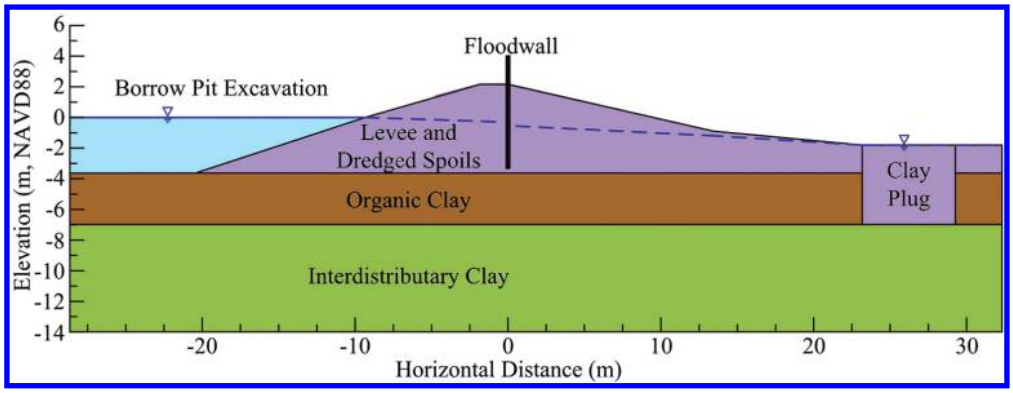

Table 2. Engineering index properties for soils in no-failure section in Fig. 5 (data from Fugro 2012).

Soil type	Soil classification (ASTM 2011*b*)	γ_{sat} (kN/m^3)	w_o (%)	LL (%)	PI (%)
Levee fill and dredged spoils	CH	16.3	43–68	73–103	21–76
Organic clay	OH	9.9–13.7	110–451	166	111
Interdistributary (ID) clay	CH	18.0	34–80	33–97	16–72

water contents, and changes in water content as a function of pore-water pressure.

Figure 5 shows the floodwall system in the no-failure section consists of a reinforced concrete floodwall and a supporting sheet pile extending to an elevation of –3.2 m NAVD88. The sheet pile impedes seepage through the levee fill and dredged spoils so the focus of the seepage analysis is flow through the organic clay layer below the sheet pile tip. The soil borrow pit or deep excavation is modeled 23 m from the floodwall. A clay plug on the landside is modeled about 25 m from the floodwall. The clay plug represents an excavation or ditch on the landside along Jourdan Avenue that was retrofitted with a reinforced concrete storm water box culvert to bury Jourdan Avenue Canal prior to Hurricane Katrina. This concrete box culvert parallels the floodwall in the Lower Ninth Ward along the length of the IHNC and was backfilled with clayey soil.

The transient model was calibrated using the 2011 Tropical Storm Lee hydrograph and field data from four landside VW pi-

ezometers located 7.6 m (25 ft) landside from the floodwall. The piezometers were installed at elevations of –2.3, –3.8, –4.7, and –8.4 m NAVD88. Rainfall infiltrating and saturating the levee fill caused pore-water pressures to increase at piezometers of elevations –2.3, –3.8, and –4.7 m NAVD88. However, the piezometer at elevation –8.4 m NAVD88 (located in the ID clay) did not measure pore-water pressure increase, which corroborates that low hydraulic conductivity and high compressibility of the organic clay does not instantaneously transmit floodside pore-water pressure to the landside toe. As a result, the calibrated transient model is used to perform a parametric analysis using k_h, m_v, and levee geometry.

Soil properties

In a saturated transient seepage analysis, three soil properties are required: (*i*) saturated k_h, (*ii*) saturated k_v/k_h ratio, and (*iii*) m_v. Table 3 provides the soil properties used for the parametric analysis of the no-failure section. The k_h and k_v/k_h were estimated from small (25.4 mm; 1 in.) and large (127 mm; 5 in.) diameter laboratory hydraulic conductivity tests (ASTM (2010) standard D5048) that were trimmed in horizontal and vertical orientations to estimate hydraulic conductivity anisotropy. The organic clay k_h was found to be between 10^{-6} and 10^{-8} cm/s, with an upper range of 10^{-5} cm/s. As a result, parametric analyses were performed using values of k_h in the 10^{-5} cm/s range. The values of m_v were computed from 1-D consolidation test results shown in Fig. 1. For each soil, average values of m_v were selected. The parametric analyses also investigated soil variability by using the lowest and highest values of m_v from Fig. 1. This represents upper and lower bounds of m_v that can influence landside uplift pressures. Observations during borrow pit excavation, numerous soil borings, cone penetration soundings, vane shear tests, and other evidence (ILIT 2006; IPET 2007) show the native soils in the borrow pit area (see Figs. 3 and 4) are representative of the IHNC soils summarized in Tables 2 and 3.

Model boundary conditions

For a transient analysis, it is essential to define the initial groundwater conditions. The initial floodside steady-state boundary condition is assumed to be a total head (h_t) boundary condition of elevation +0 m NAVD88, which represents the canal water level inside the borrow pit excavation before the 2005 hurricane. This is consistent with canal water levels measured prior to Hurricane Katrina. The initial landside steady-state boundary condition is assumed to be 0.3 m (1 ft) below the ground surface based on borings and excavations in 2011 and the Florida Avenue Pump Station. The phreatic surface and total head loss across the sheet pile wall was estimated using a steady-state analysis and the floodside and landside boundary conditions described in the preceding text. These steady-state results become the parent analysis, i.e., starting point, for the transient analyses.

The transient total head conditions applied to the floodside for this study are the 2005 Hurricane Katrina storm surge (see Fig. 6*a*) and the 2011 Mississippi River flood level (Fig. 6*b*). The data points shown in Figs. 6*a* and 6*b* were used to model these hydrographs in SEEP/W by inputting sets of data points and modeled as a floodside total head boundary. In Fig. 6*a*, the hurricane surge increased from elevation +1.4 m NAVD88 after 10 h to elevation +4.3 m NAVD88 at 25 h and then precipitously returned to elevation +0 m. Because the top of the floodwall is at elevation +4 m NAVD88 (IPET 2007), the maximum surge level was decreased to correspond with the top elevation of the floodwall and thus prevent overtopping for the parametric analyses. The 2011 Mississippi River flood — obtained from USACE river gauge at Duncan Point, Louisiana, USA — represents a long-duration flood event and is used to understand the difference in seepage conditions between a rapid storm surge and a long-duration flood event. Elevations of the Mississippi River at Duncan Point are higher than the IHNC, so the flood levels were normalized such that the peak flood elevation also corresponds to the top elevation of the floodwall or elevation +4 m NAVD88. The flood level in Fig. 6*b* reaches a first peak at elevation +2.7 m NAVD88 after 65 days and then reaches the maximum flood level of elevation +4 m NAVD88 after 100 days. For comparison purposes, the Hurricane Katrina storm surge is superimposed on the 2011 flood event in Fig. 6*b*. Figure 6*a* is a short-term event; Fig. 6*b* is a long-duration flood, so both hydrographs represent scenarios that may be present in extreme events that can impact levee design and are used to illustrate the range of landside hydraulic response.

The SEEP/W program "potential seepage face review" option was selected for the ground surface from the floodwall to landside levee toe because the phreatic surface on the landside levee slope is unknown, and the near-surface soil is unsaturated based on landside borings and excavations. If the phreatic surface increases above the elevation of landside toe, then SEEP/W treats the slope-

Table 3. Soil parameters for transient seepage analyses of no-failure section in Fig. 5 (data from Fugro 2012).

Soil type	k_h (cm/s)	k_v/k_h	m_v (kPa^{-1}) Lowest value	Average	Highest value
Levee fill and dredged spoils	1×10^{-6}	0.83	3×10^{-4}	8×10^{-4}	2×10^{-3}
Organic clay	Ranges	0.33	5×10^{-4}	1.2×10^{-3}	3×10^{-3}
Interdistributary clay	3×10^{-7}	0.50	3×10^{-4}	8×10^{-4}	2×10^{-3}

Fig. 6. Hydrographs applied in parametric study: (*a*) 2005 Hurricane Katrina at IHNC in hours; (*b*) 2011 Mississippi River flood at Duncan Point, Louisiana, in days.

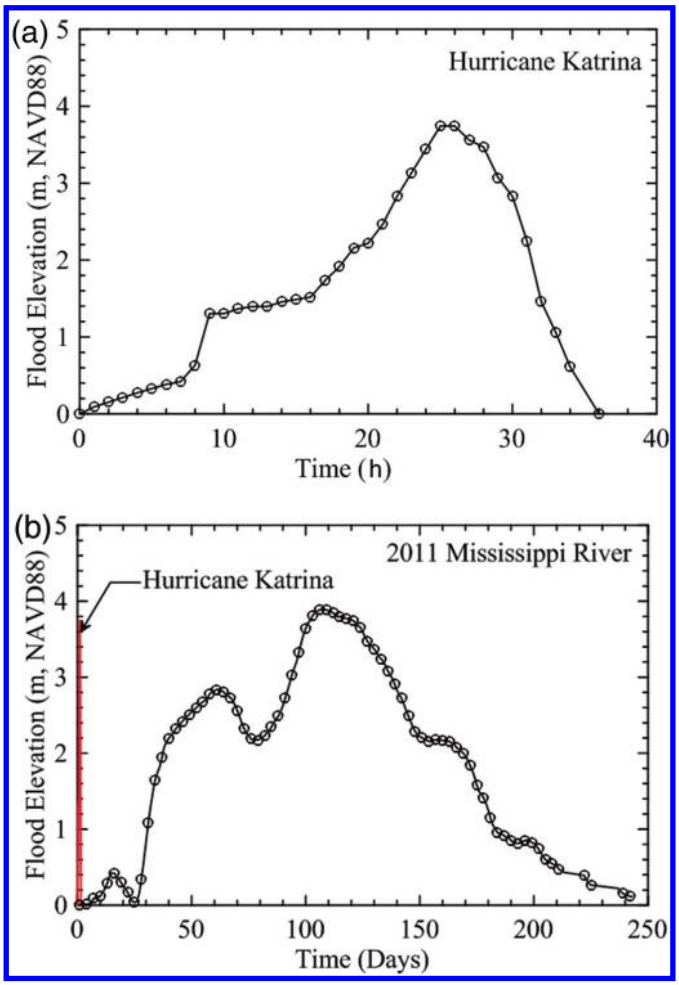

face water flow as runoff. The landside boundary condition from the landside levee toe to the RHS of finite element mesh is zero pressure head (h_p). In SEEP/W, the $h_p = 0$ boundary condition from the levee toe to the RHS of the mesh signifies that the groundwater level is at the ground surface, which is a reasonable assumption because of the normally high groundwater surface in the area coupled with the rainfall infiltration associated with the flood events. The left-hand side (LHS) vertical boundary is characterized as zero flow, which occurs at a groundwater divide. The IHNC channel was considered a groundwater divide because of symmetry of the canal channel. The RHS vertical boundary is modeled as a total head boundary (h_t = –2.0 m or about equal to the ground surface) to represent the far-field groundwater conditions. Finally, the boundary condition along the bottom of the seepage model in Fig. 5 is modeled as an impervious boundary due to the low hydraulic conductivity ID clay.

Zone of interest

Landside sand boils can form when seepage forces increase such that the effective vertical stress is zero, while heave occurs when the uplift pressures of seepage exceed the downward forces due to the submerged weight of soil. In general, the zone of interest for erosion and heave-related issues is the levee toe because it often exhibits the thinnest cover soil and is closest to the floodwall. Wolff (2002) reports that the location of sand boils or heave can also be influenced by local geologic conditions. For example, high exit gradients and concentrations of seepage are usually found along the landside toe at thin or weak spots in the top stratum and adjacent to or along clay-filled swales or channels, such as the clay plug in Fig. 5 or landside ditches. More than likely, local preferential flow paths and a thin or weak top stratum caused the large sand boils described by Wolff (2002) to develop. This study found that man-made structures (a box culvert) or clay-filled ditch can generate higher uplift pressures in the vicinity of the clay plug (see Fig. 5) than at the levee toe. This is caused by the seepage flow being impeded or blocked by the impermeable plug and seepage being forced upwards, creating large uplift pressures under the top stratum. As a result, FS against uplift is calculated on the floodside of the clay plug in Fig. 7.

Effect of coefficient of volume compressibility

Figure 7 presents the factor of safety against uplift developed using parametric values of organic clay k_h, ranging from 1×10^{-5} to 6×10^{-5} cm/s, and values of m_v. The organic clay m_v values represent the average, highest, and lowest values of 1.2×10^{-3}, 3×10^{-3}, and 5×10^{-4} kPa^{-1}, respectively, in Fig. 7. Transient seepage analyses performed using the Hurricane Katrina hydrograph exhibit almost no change in landside pore-water pressures and gradients because of the short duration of the hydrograph. Thus, the parametric analyses focus on the 2011 Mississippi River flood hydrograph. The results of varying saturated k_h are shown in Fig. 7, and the values of m_v are used to illustrate the impact on seepage through the organic clay layer. For a given m_v value, increasing the saturated k_h increases the maximum uplift pressure. The increase in uplift pressure and effect of m_v are negligible for $k_h \leq 10^{-5}$ cm/s, i.e., seepage-induced uplift pressures in the landside are generated when $k_h > 10^{-5}$ cm/s. This shows that selecting a compatible m_v value for saturated fine-grained soils with $k_h > 10^{-5}$ cm/s is critical to develop a representative transient seepage analysis. If a compatible, i.e., realistic, value of m_v is used, water must flow from the floodside to the landside of the floodwall to transmit the uplift pressures and seepage forces.

The first effect of m_v is that it can delay or accelerate, depending on the value of the onset of uplift water pressure increase at the clay plug from the initial steady-state conditions. The time for underseepage to reach the clay plug for $m_v = 3 \times 10^{-3}$ kPa^{-1} (triangle symbol in Fig. 7) is about 161 days. By decreasing the value of m_v to 1.2×10^{-3} and 5×10^{-4} kPa^{-1}, the time for underseepage to reach the clay plug decreases to about 83 days (circle symbol) and 62 days (square symbol), respectively. As a result, the time for underseepage to reach the clay plug decreases by a factor of about 2.5 times when m_v ranges from highest to lowest value and k_h remains constant. This behavior is reasonable because large m_v values increase the RHS of eq. (1), i.e., total hydraulic heads induced by the flood dissipate at a faster rate. On the contrary, a low-compressibility soil for the same time period allows less head to dissipate from the flood and thus results in uplift pressures developing quicker at the landside levee.

The second effect is that decreasing m_v increases maximum uplift pressures during the flood. For $k_h = 3 \times 10^{-5}$ cm/s, the initial steady-state uplift FS is 1.18, and it decreases during the flood to 1.15 and 1.03 for m_v of 3×10^{-3} and 5×10^{-4} kPa^{-1}, respectively. When $k_h = 6 \times 10^{-5}$ cm/s, FS decreases with time from a steady-state value of 1.08 to 0.97 and 0.85 for m_v of 3×10^{-3} and 5×10^{-4} kPa^{-1}, respectively, which indicates heave may develop according to USACE (2005). By decreasing the organic clay m_v from the highest to lowest value, i.e., 3×10^{-3} to 5×10^{-4} kPa^{-1}, FS is observed to decrease by about 10% for k_h of 3×10^{-5} and 6×10^{-5} cm/s. Based on this case study, the effect of m_v increases significantly as k_h increases to 1×10^{-4} cm/s. The results for $k_h = 1 \times 10^{-5}$ cm/s also indicate that vertical hydraulic gradients are unaffected, which is reasonable due to the low hydraulic conductivity of the organic clay.

Table 4 compares the FS against uplift at the clay plug for average m_v under transient conditions as well as assuming maximum flood surge at a steady-state condition. These gradients illustrate the influence of the saturated k_h of the organic clay layer on the vertical hydraulic gradients calculated a distance of 20 m from the floodwall. Table 4 also shows the FS values for the steady-state condition are significantly lower (about 22%) and thus more conservative than the transient FS values. Steady-state conditions may not develop during rapid events, e.g., hurricanes, storms, and river floods, so transient unsaturated seepage analyses are recommended for design of seepage control measures to understand the impact of short-duration hydrographs and values of m_v on the design of the remedial measures.

Effect of system compressibility

Figure 7 shows the value of m_v selected for the organic clay layer in Fig. 5 has a large impact on the landside uplift pressures and vertical gradients. Also important for the landside uplift pressures is the value of m_v selected for the floodwall or levee system, i.e., other layers in the cross section, such as levee fill and ID clay. Using $k_h = 3 \times 10^{-5}$ cm/s, Fig. 8 illustrates this effect on uplift FS by varying the compressibility of the other layers (system compressibility). For case 1, the organic clay layer m_v is assumed to be the highest value of 3×10^{-3} kPa^{-1}. When the system m_v is also the highest, negligible underseepage occurs in Fig. 8; thus, there is no pore-water pressure increase and no heave at the clay plug. In case 2, the system m_v is assumed to be the lowest value and a slight increase in gradients is observed, with the organic clay m_v still being the highest value. In cases 3 and 4, the system compressibility is varied and the organic clay remains constant. The system m_v is the highest value in case 3 and is the lowest value in case 4. Considering case 4 first, the system m_v is similar to case 2 but the organic clay m_v is reduced to the average value of 1.2×10^{-3} kPa^{-1}. The uplift FS decreases from 1.14 in case 2 to about 1.04 in case 4, which demonstrates that the organic clay m_v controls the induced pore-water response and observed heave. Comparing cases 3 and 4, the system m_v does influence uplift potential but does not contribute as much as the organic clay m_v. The results in Fig. 8 demonstrate that the compressibility of the layer in which seepage is occurring is more important than the other soils. However, the other values of m_v still contribute to landside uplift pressures because they can focus seepage in the layer of interest, so reason-

Fig. 7. Effect of m_v on factor of safety against uplift at clay plug in Fig. 5, using Mississippi River flood hydrograph for various values of horizontal hydraulic conductivity and compressibility.

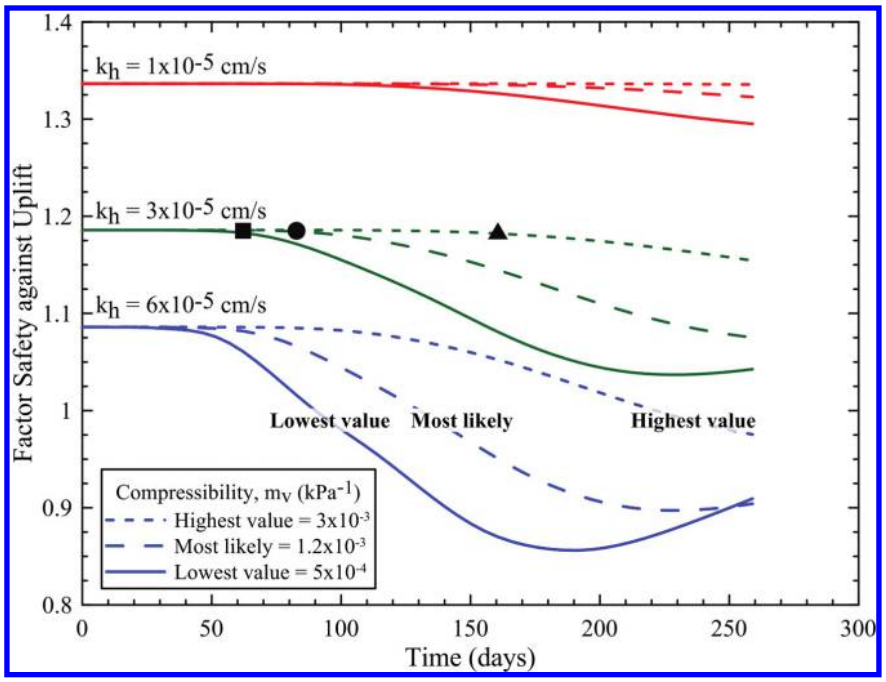

Table 4. Summary of vertical hydraulic gradients at clay plug using average of m_v and elevation +4 m (NAVD88) flood level for steady-state conditions and 2011 Mississippi River flood hydrograph.

	Factor safety against uplift		
k_h (cm/s)	Initial conditions[a]	Transient, average m_v[b]	Steady state[c]
1×10^{-5}	1.34	1.32	1.12
3×10^{-5}	1.18	1.08	0.84
6×10^{-5}	1.08	0.90	0.69

[a]River level, elevation +0 m NAVD88.
[b]Figure 6*b* hydrograph.
[c]Flood level, elevation +4 m NAVD88.

able values of m_v should be selected in the transient seepage model.

Recommendations for slope stability analyses

Performing slope stability analyses requires judgment and experience on whether a soil is drained or undrained. In most cases, stability analyses involving clays, silts, and organic clay soils are assumed undrained, while gravels, sands, and sometimes nonplastic silts are considered drained materials. When sufficient experience to correctly apply judgment is lacking, a quantitative analysis can be performed to assist in the decision. Duncan and Wright (2005) present a relationship that uses the coefficient of consolidation (c_v) and length of drainage path (H_{dr}) to determine the time required for 99% pore-water pressure dissipation (T_{99}). The T_{99} value is then compared with the duration of loading to determine if the soil behaves in a drained or undrained manner. For example, the IHNC organic clay in Fig. 5 behaves in an undrained manner during Hurricane Katrina because pore-water pressures generated from shear stresses cannot dissipate in 20–30 h. For the Mississippi River flood, the longer loading period allows pore-water pressure several months to dissipate, which may change undrained to drained conditions, depending on H_{dr}.

Identifying drained or undrained behavior requires accurate representation of the coefficient of consolidation, where $c_v = k_v/(\gamma_w m_v)$. Values of c_v should be determined from 1-D constant rate of strain or incremental stress consolidation tests conducted on high-quality samples at the in situ effective vertical stress. In some cases, values of m_v and k_v can be evaluated independently from either empirical correlations, field tests, or other laboratory tests and then used to estimate c_v. Although m_v and k_v are computed independently, Fig. 9 shows m_v and k_v are inversely related, i.e., as m_v decreases, k_v increases. For example, assuming $m_v = 1\times10^{-6}$ kPa^{-1} for a sand, the computed k_v should range from 1×10^{-3} to 1 cm/s. This range is consistent with k_v ranges reported by Terzaghi et al. (1996). As a result, the relationship shown in Fig. 9 presents a

Fig. 8. Effect of system compressibility and organic clay layer compressibility on landside uplift factors of safety.

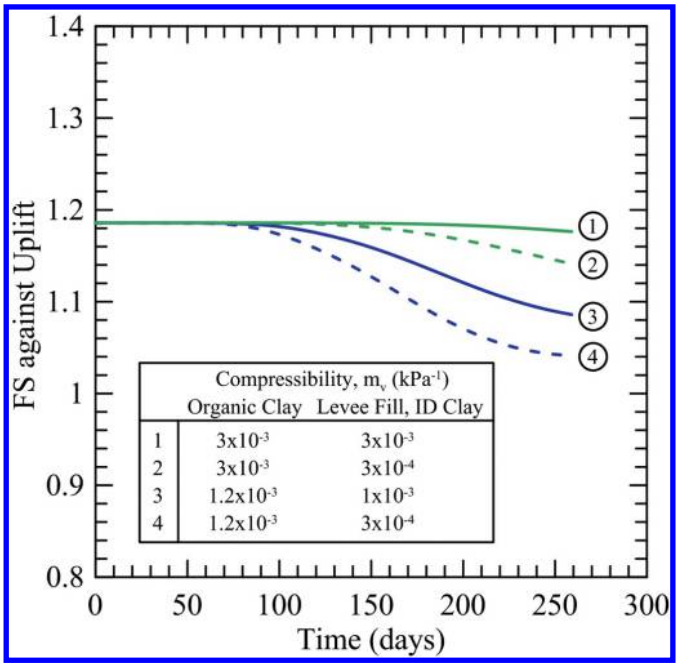

Fig. 9. Relationship between vertical saturated hydraulic conductivity and compressibility.

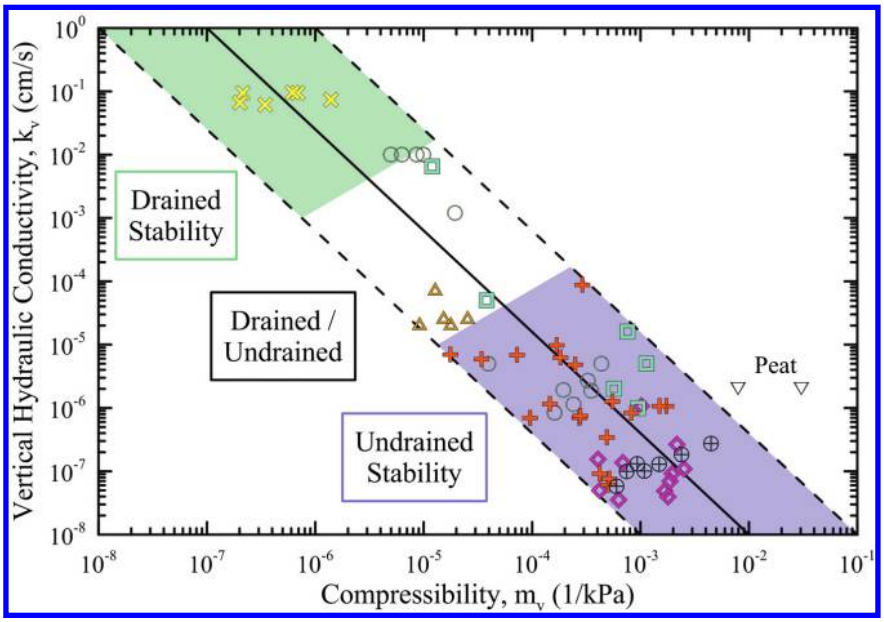

means for verifying compatible values of m_v and k_v are selected because they are estimated independently.

The m_v and k_v data in Fig. 9 vary by several orders of magnitude, which makes estimating an accurate value of c_v difficult. Alternatively, the shaded regions in Fig. 9 can be used for guidance on evaluating whether drained or undrained conditions control soil behavior. For example, gravels and sands are characterized by low compressibility and high hydraulic conductivity, i.e., $m_v = 10^{-7} - 10^{-5}$ kPa^{-1} and $k_v > 1 \times 10^{-3}$ cm/s, and thus represent the drained shaded region in the top left of Fig. 9. The shaded region representing undrained conditions corresponds to saturated fine-grained soils that are more compressible ($m_v \sim 10^{-4}$ kPa^{-1}) and less permeable ($k_v < 1 \times 10^{-6}$ cm/s). Soils such as silts and sandy clay may be drained or undrained, i.e, area between shaded regions in Fig. 9. In this case, both conditions should be investigated to cover the range of possible soil behavior.

Based on Fig. 9, an engineer can determine if an undrained or total stress stability analysis should be performed, and accordingly, undrained or total stress strengths should be used. If an undrained analysis is performed, a seepage analysis is not required in the slope stability assessment because the factor of safety is not affected by pore-water pressures calculated from the seepage analysis. In an undrained analysis, the flood loading on the ground surface, levee, and sheet pile wall are considered solely as boundary pressures. Internal pore-water pressures are not included in the analysis; therefore, the calculated factor of safety does not depend on the hydraulic conductivity or compressibility of the fine-grained soil units.

Recommendations for transient seepage analyses

The state of practice for levee design and remediation is performing a steady-state seepage analysis (USACE 1993, 2005). However, there is interest in performing transient unsaturated seepage analyses to calibrate transient seepage models with piezometric data and investigate the level of conservatism with a design based on steady-state conditions. As a result, the following procedure is recommended for such transient unsaturated seepage analyses:

1. *Initial steady-state conditions* — Before performing a transient analysis, the initial pore-water pressure regime near the levee must be determined. The floodside and landside groundwater surface before flooding or storm surge should be determined from subsurface information and used to establish the initial phreatic surface through the levee via a steady-state analysis. The initial groundwater conditions can be established via piezometer, boring, or excavation data.
2. *Selecting soil parameters* — For fine-grained, erodible soils such as silts and silty sands through which flow will occur, laboratory 1-D consolidation testing, C_c and w_o empirical correlation, and piezometer readings can be used to initially estimate m_v for transient seepage studies. Values of k_h and the anisotropy ratio of k_h/k_v should be measured using 127 mm (5 in.) laboratory permeameter tests (ASTM (2010) standard D5048) and high-quality specimens. Values of k_v and m_v can be validated for compatibility using Fig. 9 and then used to determine if drained conditions control the accompanying stability analyses.
3. *Transient seepage* — The initial steady-state pore-water pressure regime is used as a "parent analysis" or starting point for the transient analysis. The appropriate floodside hydrograph should be used for the transient boundary conditions. The analysis is performed using the median or average value of m_v based on site-specific data. Additional analyses using the highest and lowest m_v values should be performed to develop upper and lower bounds, respectively, of the magnitude of uplift pressures and vertical hydraulic gradient. In addition, the location or zone of interest for the calculated uplift pressures and vertical gradients can be determined and compared with initial estimates, e.g., levee toe, to ensure reasonable responses and design measures.
4. *Underseepage and exit gradients* — Using a graph similar to Fig. 7, the calculated uplift pressures or vertical gradients for a given k_h and m_v can be used to estimate the FS against uplift or heave, respectively. An exit hydraulic gradient of 0.85 calculated in the vertical direction on the landside of a levee is commonly considered sufficient to initiate heave and subsequent erosion, i.e., sand boils, in granular soils (USACE 2005). Other field measurements show that sand boils may occur with exit hydraulic gradients in the range of 0.54–1.02 (Daniel 1985). In cohesive soils, e.g., IHNC organic clay, sand boils will not develop, but a gradient >0.85 may be sufficient to cause some heave, provided there is a pervious layer underlying the fine-grained layer.

5. *Seepage control measures* — Using steady-state analysis results for design of cutoff walls and (or) relief wells is conservative (see Table 4), so the introduction of a transient analysis may preclude the use of a cutoff wall and only installation of relief wells.
6. *Slope stability* — To accurately model a transient condition in an effective stress stability analysis, a fully coupled stress–seepage analysis is required. The contribution of changes in total stress and shear stress on the generated pore pressures in fine-grained soil has to be included in the analysis because these are not calculated in a transient seepage analysis. Unfortunately, this fully coupled type of analysis is not common in geotechnical engineering practice (Alonso and Pinyol 2011). Transient analyses do provide guidance on when a conventional steady-state seepage stability analysis is warranted, or when a "rapid flood loading" analysis is required. Transient analyses can also provide useful information regarding porewater pressures in pervious layers that can apply destabilizing uplift pressures to the layers above.

In summary, steady-state and transient seepage are used to reflect certain boundary conditions, soil properties, e.g., high hydraulic conductivity, saturation, and compressibility, and loading conditions, e.g., short-duration flood or rapid storm surge. The user must determine the boundary conditions, soil conditions, and loading conditions that best simulate field conditions to estimate realistic seepage-induced uplift pressures and hydraulic gradients. Calibration of the transient seepage model with piezometer data and compatible values of hydraulic conductivity and compressibility is also recommended.

Summary

This paper illustrates the importance of soil compressibility on transient and unsaturated seepage analyses using a floodwall case study. This paper also provides guidance on selecting compatible values of soil compressibility and hydraulic conductivity for transient seepage analyses and the potential conservatism with a steady-state analysis. The following information and recommendations were derived from the parametric analyses:

1. The derivation of transient seepage flow indicates that reducing the value of m_v, i.e., making the system incompressible, transforms the transient seepage analysis to a steady-state analysis by essentially eliminating the effect of time on seepage. Although water is considered incompressible, the value of m_v should not be assumed to be incompressible because m_v is a function of both the soil skeleton and water compressibility.
2. The increase in landside uplift pressure and effect of m_v are significant for $k_h > 10^{-5}$ cm/s as shown in Fig. 7. This shows that selecting a compatible m_v value for saturated fine-grained soils with $k_h > 10^{-5}$ cm/s is critical to develop a representative transient seepage analysis.
3. General procedures for estimating m_v include laboratory consolidation tests, C_c empirical correlations, field calibration using piezometer data, piezometer slug tests, and field pump tests. Values of m_v vary by about an order of magnitude for the same soil type. To account for uncertainty in m_v, the average or median m_v should be used with additional analyses using the highest and lowest values, respectively, to develop lower and upper bounds of response. The selected value of m_v should also be representative of the in situ effective vertical stress and compatible with the value of hydraulic conductivity as shown in Fig. 9.
4. The parametric analyses show that values of m_v for the seepage layer and system affect the time at which landside uplift pressures start to increase and the magnitude of landside uplift pressures. In particular, the effect of m_v diminishes as the soil becomes more compressible. As expected, seepage flow must be present for uplift pressures to be generated on the landside of the levee or floodwall.
5. Performing slope stability analyses requires judgment and experience on whether a soil is drained or undrained. Figure 9 shows an inverse relationship between m_v and k_v and can be used to evaluate whether a soil will be undrained or drained under the applied loading conditions.
6. Current state of practice for levee underseepage does not require transient seepage analyses; thus, levee design based on steady-state analyses is potentially conservative. A design procedure for performing transient seepage analyses is presented herein that describes how to model initial steady-state seepage conditions before applying the design flood hydrograph, estimating transient material properties, and using the results to predict an approximate time at which underseepage distress may begin and the zone of interest for exit uplift pressures and vertical hydraulic gradients.

Acknowledgements

This material is based upon work supported by the National Science Foundation through a Graduate Research Fellowship to Navid H. Jafari. Any opinions, findings, and conclusions or recommendations expressed in this material are those of the authors and do not necessarily reflect the views of the National Science Foundation.

References

Alonso, E.E., and Pinyol, N.M. 2011. Landslides in reservoirs and dam operation. Dam Maintenance and Rehabilitation II, pp. 3–27. doi:10.1201/b10570-3.

ASTM. 2010. Standard test methods for measurement of hydraulic conductivity of saturated porous materials using a flexible wall permeameter. ASTM standard D5084. *In* 2010 Annual Book of ASTM Standards, Vol. 04.08. American Society for Testing and Materials, Philadelphia.

ASTM. 2011*a*. Standard test methods for one-dimensional consolidation properties of soils using incremental loading. ASTM standard D2435. *In* 2011 Annual Book of ASTM Standards, Vol. 04.08. American Society for Testing and Materials, Philadelphia.

ASTM. 2011*b*. Standard practice for classification of soils for engineering purposes (Unified Soil Classification System. ASTM standard D2487. *In* 2011 Annual Book of ASTM Standards, Vol. 04.08. American Society for Testing and Materials, Philadelphia.

ASTM. 2012. Standard test method for one-dimensional consolidation properties of saturated cohesive soils using controlled-strain loading (D4186). *In* 2012 Annual Book of ASTM Standards, Volume 04.08. American Society for Testing and Materials, Philadelphia.

Bell, F.G. 2000. Engineering properties of soils and rocks. 4th ed. Blackwell Science, UK.

Bennett, P.T. 1946. The effect of blankets on seepage through pervious foundations. (Paper No. 2270.) Transactions of the American Society of Civil Engineering, **111**(1): 215–228.

Berilgen, M. 2007. Investigation of stability of slopes under drawdown conditions. Computers and Geotechnics, **34**: 81–91. doi:10.1016/j.compgeo.2006.10.004.

Borja, R.I., and Kishnani, S.S. 1992. Movement of slopes during rapid and slow drawdown. *In* Stability and performance of slopes and embankments — II. *Edited by* R.S. Seed and R.W. Boulanger. Geotechnical Special Publication No. 31. American Society of Civil Engineers. pp. 404–413.

Brahma, S.P., and Harr, M.E. 1962. Transient development of the free surface in a homogeneous earth dam. Géotechnique, **12**: 283–302. doi:10.1680/geot.1962.12.4.283.

Browzin, B.S. 1961. Non-steady flow in homogeneous earth dams after rapid drawdown. *In* Proceedings of the 5th International Conference on Soil Mechanics and Foundations, Paris. Vol. 2, pp. 551–554.

Casagrande, A. 1937. Seepage through dams. New England Water Works. Vol. II, No. 2.

Casagrande, A. 1961. Control of seepage through foundations and abutments of dams. 1st Rankine Lecture. Géotechnique, **11**(3): 161–182. doi:10.1680/geot.1961.11.3.161.

Cedergren, H.R. 1989. Seepage, drainage, and flow nets. John Wiley and Sons, N.Y.

Chapuis, R.P., and Aubertin, M. 2001. A simplified method to estimate saturated and unsaturated seepage through dikes under steady-state conditions. Canadian Geotechnical Journal, **38**(6): 1321–1328. doi:10.1139/t01-068.

Chen, Q., and Zhang, L.M. 2006. Three-dimensional analysis of water infiltration into the Gouhou rockfill dam using saturated–unsaturated seepage theory. Canadian Geotechnical Journal, **43**(5): 449–461. doi:10.1139/t06-011.

Cooley, R.L. 1983. Some new procedures for numerical solution of variably sat-

urated flow problems. Water Resources Research, **19**(5): 1271–1285. doi:10.1029/WR019i005p01271.
Cunny, R.W. 1980. Documentation and analysis of rock island underseepage data. U.S. Army Corps of Engineers Waterways Experiment Station, Technical Report GL-80-3. U.S. Army Corps of Engineers, Vicksburg, Miss.
Daniel, D.E. 1985. Review of piezometric data for various ranges in the rock island district. USACE Waterways Experiment Station, U.S. Army Corps of Engineers, Vicksburg, Miss.
Desai, C.S. 1972. Seepage analysis of earth banks under drawdown. Journal of the Soil Mechanics and Foundations Division, ASCE, **98**(11): 1143–1162.
Desai, C.S. 1977. Drawdown analysis of slopes by numerical method. Journal of the Geotechnical Engineering Division, ASCE, **103**(7): pp. 667–676.
Desai, C.S., and Sherman, W.C. 1971. Unconfined transient seepage in sloping banks. Journal of the Soil Mechanics and Foundations Division, ASCE, **97**(2): 357–373.
Domenico, P.A., and Mifflin, M.D. 1965. Water from low-permeability sediments and land subsidence. Water Resources Research, American Geophysical Union, **1**(4): 563–576. doi:10.1029/WR001i004p00563.
Duncan, J.M., and Wright, S.G. 2005. Soil strength and slope stability. John Wiley & Sons, Inc., N.J.
Duncan, J.M., Wright, S.G., and Wong, K.S. 1990. Slope stability during rapid drawdown. *In* Proceedings of the Seed Memorial Symposium, BiTech Publishers, Ltd., Vancouver, B.C. Vol. 2, pp. 235–272.
Fredlund, D.G., and Rahardjo, H. 1993. Soil mechanics for unsaturated soils. John Wiley & Sons, Inc., N.J.
Freeze, R.A., and Cherry, J.A. 1979. Groundwater. Prentice-Hall Inc., Englewood Cliffs, N.J.
Fugro. 2012. Geotechnical data report, Inner Harbor Navigational Canal, East Bank Industrial Area (IHNC-EBIA), field & laboratory testing program. Final report. New Orleans, La. Report No. 04.57114007-2.
Gabr, M.A., Wolff, T., Taylor, H., and Brizendine, A. 1996. Underseepage analysis of levees on two-layer and three-layer foundation. Computers and Geotechnics, **18**(2): 85–107. doi:10.1016/0266-352X(95)00024-5.
Geo-Slope International. 2007. Seep/W software users guide. Geo-Slope International Ltd., Calgary, Alta.
Holtz, R.D., and Kovacs, W.D. 1981. An introduction to geotechnical engineering. Prentice-Hall, Inc., Englewood Cliffs, N.J.
Independent Levee Investigation Team (ILIT). 2006. Investigation of the performance of the New Orleans regional flood protection systems during Hurricane Katrina. Final report. Available from http://www.ce.berkeley.edu/new_orleans/ [accessed 31 July 2006].
Interagency Performance Evaluation Task Force (IPET). 2007. Performance evaluation of the New Orleans and southeast Louisiana hurricane protection system. Final Report of the Interagency Performance Evaluation Task Force. U.S. Army Corps of Engineers. Available from http://media.nola.com/hurricane_katrina/other/060106corps_vol7.pdf.
Kulhawy, F.H., Duncan, J.M., and Seed, H.B. 1969. Finite element analysis of stresses and movements in embankments during construction. Report No. S-69-8. U.S. Army Engineer Waterways Experiment Station, U.S. Army Corps of Engineers, Vicksburg, Miss.
Lam, L., and Fredlund, D.G. 1984. Saturated-unsaturated transient finite element seepage model for geotechnical engineering. Advances in Water Resources, **7**: 132–136. doi:10.1016/0309-1708(84)90042-3.
Lam, L., Fredlund, D.G., and Barbour, S.L. 1987. Transient seepage model for saturated-unsaturated soil systems: a geotechnical engineering approach. Canadian Geotechnical Journal, **24**(4): 565–580. doi:10.1139/t87-071.
Lambe, T.W., and Whitman, R.V. 1969. Soil mechanics. John Wiley & Sons, N.Y.
Lane, P., and Griffiths, D. 2000. Assessment of stability of slopes under drawdown conditions. Journal of Geotechnical and Geoenvironmental Engineering. **126**(5): 443–450. doi:10.1061/(ASCE)1090-0241(2000)126:5(443).
Le, T., Gallipoli, D., Sanchez, M., and Wheeler, S.J. 2012. Stochastic analysis of unsaturated seepage through randomly heterogeneous earth embankments. International Journal for Numerical and Analytical Methods in Geomechanics, **36**(8): 1056–1076. doi:10.1002/nag.1047.
Li, G.C., and Desai, C.S. 1983. Stress and seepage analysis of earth dams. Journal of Geotechnical Engineering, **109**(7): 946–960. doi:10.1061/(ASCE)0733-9410(1983)109:7(946).
Mansur, C.I., and Kaufman, R.I. 1957. Underseepage-Mississippi River Levees. St. Louis District. Transactions of the ASCE, **122**.
Mansur, C.I., Kaufman, R.I., and Schultz, J.R. 1956. Investigation of underseepage and its control, lower Mississippi River levees. Technical Memorandum No. TM 3-424. USACE Waterways Experiment Station, U.S. Army Corps of Engineers, Vicksburg, Miss.
Mansur, C.I., Postol, G., and Salley, J.R. 2000. Performance of relief well systems along Mississippi River levees. Journal of Geotechnical and Geoenvironmental Engineering, **126**(8): 727–738. doi:10.1061/(ASCE)1090-0241(2000)126:8(727).
Mesri, G., and Ajlouni, M. 2007. Engineering properties of fibrous peats. Journal of Geotechnical and Geoenvironmental Engineering, **133**(7): 850–866. doi:10.1061/(ASCE)1090-0241(2007)133:7(850).
Newlin, C.W., and Rossier, S.C. 1967. Embankment drainage after instantaneous drawdown. Journal of the Soil Mechanics and Foundations Division, ASCE, **93**(SM6): 79–96.
Nobari, E.S., and Duncan, J.M. 1972. Effects of reservoir filling on stresses and movements in earth and rockfill dams. Report No. S-72-2. U.S. Army Engineer Waterways Experiment Station, U.S. Army Corps of Engineers, Vicksburg, Miss.
Paton, J., and Semple, N.G. 1961. Investigation of the stability of an earth dam subjected to rapid drawdown including details of pore pressure recorded during a controlled drawdown test. *In* Pore pressure and suction in soils. Butterworth, London. pp. 85–90.
Peter, P. 1982. Canal and river levees. Developments of civil engineering. Vol. 29. Elsevier/North-Holland, Inc., New York.
Pinyol, N.M., Alonso, E.E., and Olivella, S. 2008. Rapid drawdown in slopes and embankments. Water Resources Research, **44**(5). doi:10.1029/2007 WR006525.
Rushton, K.R., and Redshaw, S.C. 1979. Seepage and groundwater flow: Numerical analysis by analog and digital methods. Wiley, Chichester, UK.
Terzaghi, K., Peck, R.B., and Mesri, G. 1996. Soil mechanics in engineering practice. John Wiley & Sons, N.Y.
Turnbull, W.J., and Mansur, C.I. 1961. Investigation of underseepage – Mississippi River levees. Transactions of the ASCE, **126**: 1486–1539.
URS. 2011. Remediation of floodwalls on the 17th Street Canal. OFC-05. Department of the Army, Washington, D.C.
USACE. 1993. Seepage analysis and control for dams. EM 1110-2-1901. U.S. Army Corps of Engineers (USACE), Department of the Army, Washington, D.C.
USACE. 2000. Engineering and design—design and construction of levees. EM 1110-2-1913. U.S. Army Corps of Engineers (USACE), Department of the Army, Washington, D.C.
USACE. 2005. Design guidance for levee underseepage. ETL 1110-2-569 U.S. Army Corps of Engineers (USACE). Department of the Army, Washington, D.C.
WGI. 2001. RECAP submittal report-borrow pit report. Inner Harbor Navigation Canal-East Bank Industrial Area New Orleans, La. Prepared by Washington Group International (WGI.) for the U.S. Army Corps of Engineers, New Orleans District, La.
WGI. 2005. Post-NFAATT groundwater characterization report. Inner Harbor Navigation Canal, East Bank Industrial Area. Washington Group International, Inc. (WGI).
Wink, Incorporated. 2005. Map of survey – East Bank Industrial Area. Prepared for Washington Group International.
Wolff, T.F. 1974. Performance of underseepage control measures during the 1973 Mississippi River Flood, Columbia levee district, Illinois. M.Sc. thesis, Oklahoma State University, Stillwater, Okla.
Wolff, T.F. 1989. Levee underseepage analysis for special foundation conditions. Research Report REME-GT-11. U.S. Army Corps of Engineers Waterways Experiment Station, U.S. Army Corps of Engineers Vicksburg, Miss.
Wolff, T.F. 2002. Design and performance of underseepage controls: A critical review. Report ERDC/GSL TR-02-19. U.S. Army Corps of Engineers, Engineer Research and Development Center, Vicksburg, Miss.
Zaradny, H. 1993. Groundwater flow in saturated and unsaturated soil. Balkema, Rotterdam.